OPEN

Optimal Brain ^{99m}Tc–Ethyl Cysteinate Dimer SPECT Imaging and Analysis to Detect Misery Perfusion on ^{15}O PET Imaging in Patients With Chronic Occlusive Disease of Unilateral Major Cerebral Artery

Yoshiyasu Matsumoto, MD, Kohki Oikawa, MD, Jun-ichi Nomura, MD, Daigo Kojima, MD, Sotaro Oshida, MD, Masakazu Kobayashi, MD, Kazunori Terasaki, PhD, Yoshitaka Kubo, MD, and Kuniaki Ogasawara, MD

Purpose: Misery perfusion is defined as marginally sufficient cerebral blood supply relative to cerebral metabolic demand. The aim of the present study was to determine the optimal brain ^{99m}Tc–ethyl cysteinate dimer (ECD) SPECT imaging and analysis to detect misery perfusion on ^{15}O PET imaging in patients with chronic occlusive disease of unilateral internal carotid or middle cerebral artery (MCA).

Methods: For 97 patients, cerebral blood flow, cerebral metabolic rate of oxygen, and oxygen extraction fraction were measured using ^{15}O PET; ^{99m}Tc-ECD SPECT was performed using dynamic scanning with a scan duration of 10 minutes each for 50 minutes after tracer administration. A region of interest was placed in the bilateral MCA territories and in the bilateral cerebellar hemispheres in all standardized images using a 3-dimensional stereotaxic region-of-interest template and affected-to-contralateral asymmetry ratio in the MCA territory (AR_{MCA}) and contralateral-to-affected asymmetry ratio in the cerebellar hemisphere (AR_{cbl}) were calculated.

Results: The AR_{MCA} or AR_{cbl} on ^{99m}Tc-ECD SPECT with a scan time of 20 to 30 minutes after tracer administration ($AR_{MCA20–30}$ or $AR_{cbl20–30}$) was correlated with AR_{MCA} on PET cerebral blood flow (r = 0.654) or AR_{MCA} on PET cerebral metabolic rate of oxygen (r = 0.576), respectively, more strongly than with other scan times. The area under the receiver operating characteristic curve for detecting abnormally elevated AR_{MCA} on PET oxygen extraction fraction was significantly greater for $AR_{cbl20–30}$/$AR_{MCA20–30}$ (0.947) than for $AR_{MCA20–30}$ alone (0.780) (difference between areas, 0.167; P = 0.0001) on ^{99m}Tc-ECD SPECT.

Conclusions: Combination of asymmetries in the cerebellar and cerebral hemispheres on ^{99m}Tc-ECD SPECT in a scan time of 20 to 30 minutes after tracer administration optimally detects misery perfusion in unilateral internal carotid artery or MCA occlusive disease.

Key Words: ^{99m}Tc-ECD, crossed cerebellar hypoperfusion, misery perfusion, SPECT

(*Clin Nucl Med* 2017;42: 499–505)

Misery perfusion is defined as marginally sufficient cerebral blood supply relative to cerebral metabolic demand.[1] This condition occurs in patients with occlusive diseases of the major cerebral arteries (internal carotid artery [ICA] or middle cerebral artery [MCA]). An increased oxygen extraction fraction (OEF)[1] as measured with PET indicates misery perfusion. A recent study demonstrated that increased OEF is still a predictor of a future stroke despite recent improvements in medical treatment for secondary prevention of stroke in patients with symptomatic chronic ICA or MCA occlusive diseases.[2] In addition, preoperative increased OEF reportedly predicts development of adverse events including cerebral ischemia or cerebral hyperperfusion syndrome during or after carotid endarterectomy or carotid stenting for cervical ICA stenosis.[3,4]

A cerebral hemisphere with misery perfusion due to ipsilateral ICA or MCA occlusive disease essentially exhibits a reduction in cerebral blood flow (CBF)[5] that can be detected using brain perfusion SPECT. However, misery perfusion cannot be strictly detected using brain perfusion SPECT because measurement of cerebral metabolic rate of oxygen ($CMRO_2$) is necessary for calculation of OEF. Reduced blood flow in the cerebellar hemisphere contralateral to a supratentorial lesion is defined as crossed cerebellar hypoperfusion (CCH)[6] and can be observed with brain perfusion SPECT.[6–9] Crossed cerebellar hypoperfusion occurs because of transneural metabolic depression and functional deafferentation of 1 cerebellar hemisphere due to a decrease in activity in the opposite cerebral hemisphere via the cerebropontocerebellar pathway.[8,9] In unilateral ICA occlusive disease, asymmetric blood flow in the contralateral-to-affected side of the cerebellar hemisphere indicates the cerebral metabolic rate of oxygen ($CMRO_2$) of the affected cerebral hemisphere compared with the $CMRO_2$ of the opposite cerebral hemisphere.[10] Oxygen extraction fraction is a function of $CMRO_2$/CBF. Therefore, the ratio of blood flow asymmetry on the contralateral-to-affected side in the cerebellar hemisphere to blood flow asymmetry on the affected-to-contralateral side in the cerebral hemisphere may indicate asymmetry in the affected-to-contralateral side OEF in the cerebral hemisphere. If so, misery perfusion could be observed with brain perfusion SPECT.[11]

^{99m}Tc-labeled ethyl cysteinate dimer (ECD), an accumulative radioligand, is used worldwide as a brain perfusion tracer for SPECT to investigate the pathophysiology of several neurological diseases. Several investigators have used ^{99m}Tc-ECD SPECT to

Received for publication September 9, 2016; revision accepted February 27, 2017.
From the Department of Neurosurgery and Cyclotron Research Center, Iwate Medical University, Morioka, Japan.
Conflicts of interest and sources of funding: This work was partly supported by a Grant-in-Aid for Strategic Medical Science Research from the Ministry of Education, Culture, Sports, Science and Technology of Japan (S1491001) and Scientific Research from Japan Society for the Promotion of Science (JP15K10313).
Correspondence to: Kuniaki Ogasawara, MD, Department of Neurosurgery, Iwate Medical University, 19-1 Uchimaru, Morioka, 020-8505 Japan. E-mail: kuogasa@iwate-med.ac.jp.

ISSN: 0363-9762/17/4207–0499
DOI: 10.1097/RLU.0000000000001670

image reduced blood flow in the cerebral hemisphere with unilateral ICA or MCA occlusive disease and have demonstrated that ^{99m}Tc-ECD SPECT images showed less affected-to-contralateral side asymmetry in the cerebral hemispheres than CBF PET images.[12,13] Shimosegawa et al[12] have also shown that such affected-to-contralateral side asymmetry on ^{99m}Tc-ECD SPECT images at 1 minute after tracer administration is mostly correlated with asymmetry on CBF PET images; 15 minutes later, the coefficient for the correlation decreases considerably. However, sample sizes of these studies were small (10–20 subjects), and SPECT imaging with such a short scanning duration (1 minute) is not clinically practical. Furthermore, whether the presence or absence of misery perfusion can be inferred on ^{99m}Tc-ECD SPECT images in patients with unilateral ICA or MCA occlusive disease remains uninvestigated.

The aim of the present study was to determine optimal brain ^{99m}Tc-ECD SPECT imaging and analysis parameters to detect misery perfusion on ^{15}O PET imaging in patients with chronic occlusive disease of the unilateral ICA or MCA. We used a large sample size and performed 3 studies: (1) comparison of affected-to-contralateral side asymmetry in the cerebral hemispheres on CBF PET and asymmetry on ^{99m}Tc-ECD SPECT for every scan time after tracer administration, (2) comparison of affected-to-contralateral side asymmetry in the cerebral hemispheres on $CMRO_2$ PET and contralateral-to-affected side asymmetry in the cerebellar hemispheres on ^{99m}Tc-ECD SPECT for every scan time after tracer administration, and (3) comparison of affected-to-contralateral side asymmetry in the cerebral hemispheres measured by OEF PET and asymmetry on ^{99m}Tc-ECD SPECT or the ratio of contralateral-to-affected side asymmetry in the cerebellar hemispheres to affected-to-contralateral side asymmetry in the cerebral hemispheres on ^{99m}Tc-ECD SPECT using the optimal scan time after tracer administration.

METHODS

Patients

Patients who met the following inclusion criteria were prospectively enrolled into the present study: presence of clinical symptoms suggesting ischemic episodes in the MCA or ICA territory within 3 months before visiting our institute; absence of clinical symptoms suggesting ischemic episodes in the vertebrobasilar territory; useful residual function (modified Rankin disability scale 0, 1, or 2); presence of unilateral MCA or ICA stenosis (>70% for the ICA, >50% for the MCA) or occlusion on cerebral angiography using arterial catheterization, computed tomography, or MRI; absence of occlusion or stenosis of greater than 50% in the contralateral ICA, contralateral MCA, basilar artery, and vertebral arteries; no infarct or only subcortical abnormalities (excluding infarcts involving the posterior limb of the internal capsule) in the MCA territory of the affected cerebral hemisphere on T1-, T2-, and diffusion-weighted MRI; absence of gross morphological alterations including ischemic lesions or atrophy in the cerebellum and brain stem on T1-, T2-, and diffusion-weighted MRI; and provision of written informed consent.

This protocol was reviewed and approved by our institutional ethics committee, and written informed consent was obtained from all patients or their next of kin.

Brain ^{99m}Tc-ECD SPECT Study

One to 3 months after the last ischemic episode, ^{99m}Tc-ECD SPECT studies were performed using a ring-type SPECT scanner (Headtome-SET080; Shimadzu Corp, Kyoto, Japan), which provides 31 tomographic images simultaneously. The spatial resolution of the scanner with a low-energy, all-purpose collimator was 13-mm full width at half maximum (FWHM) at the center of the field of view, and the slice thickness was 25-mm FWHM at the field-of-view center. Image slices were taken at 10-mm center-to-center spacing parallel to the orbitomeatal line. The images were reconstructed using the weighted-filtered backprojection technique, in which attenuation correction was made by detecting the edge of the object. An attenuation coefficient of 0.075 cm^{-1}, a Butterworth filter (cutoff = 0.28 cycle/cm, order = 4), and a ramp filter were used for image reconstruction.

Each patient was given an intravenous bolus injection of 740 MBq ^{99m}Tc-ECD as a commercially supplied kit. Dynamic scanning with the previously mentioned collimator was started simultaneously and continued for a total of 50 minutes (50 scans) with a scanning duration of 1 minute. Next, the 50 dynamic scans obtained in each patient were combined with a scanning duration of 10 minutes as follows: 0 to 10 minutes, 10 to 20 minutes, 20 to 30 minutes, 30 to 40 minutes, and 40 to 50 minutes after tracer administration.

Brain ^{15}O Gas PET Study

PET studies were performed 2 to 6 days before SPECT studies using a SET-3000GCT/M scanner (PET/CT; Shimadzu Corp).[14] This modality uses gadolinium silica oxide detectors and provides 59 slices with 2.6-mm slice thickness. The axial field of view was 156 mm, and the spatial resolution was 3.5-mm FWHM at 1 cm in-plane and 4.2-mm FWHM at the center axially. The scanner was operated in a static scan mode with dual-energy window acquisition for scatter correction. The coincidence time window was set to 10 nanoseconds. A shield module consisting of 7-mm-thick lead plates was attached to the gantry bed and was used to cover the breast and shoulder of the subject to reduce the counting rate of random coincidence and scatter coincidence attributable to radioactivity outside the field of view.

Before the emission scan, a transmission scan (3 minutes) with a ^{137}Cs point source was performed with a bismuth germanate transmission detector ring coaxially attached to the gadolinium silica oxide emission detector ring. Cerebral blood flow was determined while the subject continuously inhaled $C^{15}O_2$ through a mask. Measurements of $CMRO_2$ and OEF were obtained during continuous inhalation of $^{15}O_2$. Data were collected for 5 minutes. Cerebral blood flow, $CMRO_2$, and OEF were calculated using the steady-state method.[15] According to Lammertsma and Jones,[16] these last 2 values are overestimated compared with values measured using arteriovenous difference techniques. This overestimation is theoretically due to the signal from nonextracted intravascular ^{15}O.[16] To correct for this intravascular component, patients took a single breath of $C^{15}O$ to measure cerebral blood volume, and $CMRO_2$ and OEF were corrected according to cerebral blood volume.[16]

Data Analysis

All SPECT and PET images were transformed into the standard brain size and shape by linear and nonlinear transformation using SPM2 for anatomic standardization.[17] Thus, brain images from all subjects had the same anatomic format. Three hundred eighteen constant regions of interest (ROIs) were automatically placed in both the cerebral and cerebellar hemispheres using a 3-dimensional stereotaxic ROI template.[18] The ROIs were grouped into 10 segments (callosomarginal, pericallosal, precentral, central, parietal, angular, temporal, posterior, hippocampus, and cerebellar) in each hemisphere according to the arterial supply. Five (precentral, central, parietal, angular, and temporal) of these 10 segments were combined and defined as an ROI perfused by the MCA (Fig. 1). The mean value of radioactive counts on ^{99m}Tc-ECD SPECT images for each 10-minute scan time after tracer administration was

FIGURE 1. Diagrams showing some ROIs of a 3-dimensional stereotaxic ROI template on brain SPECT and PET. The white ROIs indicate the bilateral cerebellar hemispheres and cortical territories perfused by the bilateral MCAs.

measured in the bilateral MCA and cerebellar hemispheric ROIs; the mean values of CBF, $CMRO_2$, and OEF on PET images were measured in the bilateral MCA ROIs. Then, for each patient, the asymmetry ratio in the MCA ROI (AR_{MCA}) was calculated as follows: the value in the cerebral hemisphere ipsilateral to the side of the stenosed or occluded artery divided by the value in the contralateral cerebral hemisphere. The asymmetry ratio in the cerebellar hemispheric ROI (AR_{cbl}) was calculated as follows: the value in the cerebellar hemisphere contralateral to the side of the stenosed or occluded artery divided by the value in the ipsilateral cerebellar hemisphere.

Using the same method, 10 healthy subjects were studied to obtain control values: the mean and SD of AR_{MCA} on OEF PET were 1.001 and 0.044, respectively.[11] An abnormally elevated AR_{MCA} on OEF PET was defined as a value greater than the mean ± 2 SDs (1.089) obtained in these healthy subjects.[11]

Statistical Analysis

Data are expressed as the mean ± SD. Correlations between various parameters were determined using linear regression analysis and by computing regression equations and correlation coefficients, and the function of better fit was determined. When 95% confidence intervals (CIs) of correlation coefficients did not overlap each other, these correlation coefficients were defined as statistically different. The accuracy of AR_{MCA} or AR_{cbl}/AR_{MCA} on ^{99m}Tc-ECD SPECT to detect abnormally elevated AR_{MCA} on OEF PET was determined by a receiver operating characteristic (ROC) curve. Pairwise comparisons between the area under the ROC curve for AR_{MCA} on ^{99m}Tc-ECD SPECT and that for AR_{cbl}/AR_{MCA} on ^{99m}Tc-ECD SPECT were performed as proposed by Pepe and Longton.[19] Statistical significance was set at the $P < 0.05$ level. Exact 95% CI of sensitivity, specificity, and positive and negative predictive values were computed using the binomial distributions. When the 95% CIs of the sensitivity, specificity, or positive or negative predictive value for detection of an abnormally elevated AR_{MCA} on OEF PET did not overlap between AR_{MCA} and AR_{cbl}/AR_{MCA} on ^{99m}Tc-ECD SPECT, each value was defined as statistically different.

RESULTS

A total of 97 patients met the inclusion criteria and were enrolled in the present study. The mean age of the 97 patients (31 women and 66 men) was 62 ± 10 years (range, 41–76 years). Forty and 57 patients had experienced only transient ischemic attacks and minor complete strokes with or without transient ischemic attacks, respectively. Fifty, 10, and 37 patients underwent cerebral angiography using arterial catheterization, computed tomography alone, and MRI alone, respectively. These angiography studies demonstrated ICA stenosis in 25 patients, ICA occlusion in 43 patients, MCA stenosis in 15 patients, and MCA occlusion in 14 patients.

TABLE 1. Correlation Coefficients Between ECD SPECT and CBF or $CMRO_2$ PET in Patients

		SPECT Scan Time After ^{99m}Tc-ECD Administration				
		0–10 min	10–20 min	20–30 min	30–40 min	40–50 min
AR_{MCA} on ECD SPECT vs AR_{MCA} on CBF PET	Correlation coefficient	0.607	0.616	0.654	0.632	0.635
	95% CI	0.465–0.719	0.475–0.725	0.524–0.755	0.496–0.738	0.499–0.740
	P	<0.0001	<0.0001	<0.0001	<0.0001	<0.0001
AR_{cbl} on ECD SPECT vs AR_{MCA} on $CMRO_2$ PET	Correlation coefficient	0.512	0.534	0.576	0.554	0.550
	95% CI	0.342–0.646	0.371–0.666	0.426–0.696	0.396–0.681	0.389–0.676
	P	<0.0001	<0.0001	<0.0001	<0.0001	<0.0001

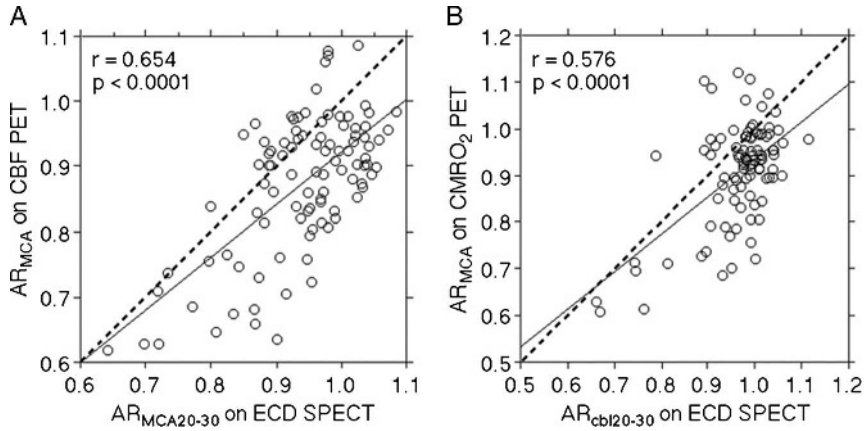

FIGURE 2. Correlation between AR_{MCA} on CBF PET and AR_{MCA} on ^{99m}Tc-ECD SPECT with a scan time of 20 to 30 minutes after tracer administration ($AR_{MCA20–30}$) in patients (**A**). Correlation between AR_{MCA} on $CMRO_2$ PET and the AR_{cbl} on ^{99m}Tc-ECD SPECT with a scan time of 20 to 30 minutes after tracer administration ($AR_{cbl20–30}$) in patients (**B**). The solid line ($y = 0.803x \pm 0.119$ for left graph; $y = 0.805x \pm 0.130$ for right graph) and dashed line are the regression line of patients and the line of identity, respectively. Each circle represents 1 patient.

The mean ± SD of AR_{MCA} on CBF and $CMRO_2$ PET in patients was 0.874 ± 0.107 (range, 0.619–1.086) and 0.905 ± 0.111 (range, 0.607–1.119), respectively. Table 1 shows correlation coefficients between values on ^{99m}Tc-ECD SPECT and those on PET in patients. Asymmetry ratio in the MCA ROI on ^{99m}Tc-ECD SPECT in all scan times after tracer administration significantly was significantly correlated with AR_{MCA} on CBF PET. The correlation coefficient for AR_{MCA} on ^{99m}Tc-ECD SPECT with a scan time of 20 to 30 minutes after tracer administration ($AR_{MCA20–30}$) was greater than that for other scan times, but a significant difference among each correlation coefficient was not observed. In most patients, $AR_{MCA20–30}$ on ^{99m}Tc-ECD SPECT was greater than AR_{MCA} on CBF PET (Fig. 2, left graph). Asymmetry ratio in the cerebellar hemisphere on ^{99m}Tc-ECD SPECT for all scan times after tracer administration was significantly correlated with AR_{MCA} on $CMRO_2$ PET (Table 1). The correlation coefficient for AR_{cbl} on ^{99m}Tc-ECD SPECT with a scan time of 20 to 30 minutes after tracer administration ($AR_{cbl20–30}$) was greater than that for other scan times, but a significant difference among each correlation coefficient was not observed. In most patients, $AR_{cbl20–30}$ on ^{99m}Tc-ECD SPECT was also greater than AR_{MCA} on $CMRO_2$ PET (Fig. 2, right graph).

The mean ± SD of AR_{MCA} on OEF PET in patients was 1.034 ± 0.083 (range, 0.924–1.475). Figure 3 shows a comparison of AR_{MCA} on OEF PET and $AR_{MCA20–30}$ and $AR_{cbl20–30}$/$AR_{MCA20–30}$ on ^{99m}Tc- ECD SPECT, respectively, for each patient. The fit to the linear regression line of the values was significant for the $AR_{MCA20–30}$ ($r = -0.218$ [95% CI, −0.400 to −0.020]; $P = 0.0316$) and the $AR_{cbl20–30}/AR_{MCA20–30}$ ($r = 0.474$ [95% CI, 0.303–0.615]; $P < 0.0001$). Of 97 patients studied, 17 were defined as having abnormally elevated AR_{MCA} on OEF PET.

Figure 4 shows a comparison of ROC curves for $AR_{MCA20–30}$ and $AR_{cbl20–30}/AR_{MCA20–30}$ on ^{99m}Tc-ECD SPECT for detecting abnormally elevated AR_{MCA} on OEF PET. The area under the

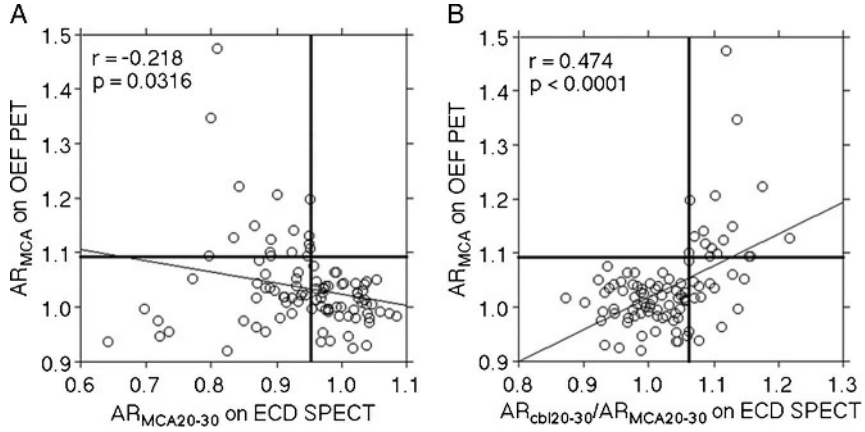

FIGURE 3. Correlation between AR_{MCA} on OEF PET and $AR_{MCA20–30}$ (**A**) or $AR_{cbl20–30}/AR_{MCA20–30}$ (**B**) on ^{99m}Tc-ECD SPECT in patients. The horizontal line denotes mean ± 2 SDs for AR_{MCA} on OEF PET obtained in healthy volunteers (a patient value greater than this line is defined as an abnormally elevated AR_{MCA} on OEF PET). The vertical line denotes the cutoff point that is closest to the left upper corner of the ROC curve for detecting abnormally elevated AR_{MCA} on OEF PET in patients. The solid line ($y = -0.203x \pm 1.226$ for **A**; $y = 0.584x \pm 0.434$ for **B**) denotes the regression line of patients. Each circle represents 1 patient.

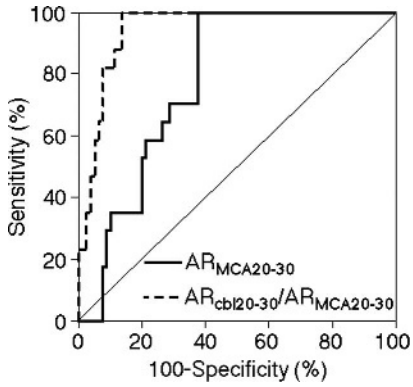

FIGURE 4. Receiver operating characteristic curves used to compare accuracy between $AR_{MCA20–30}$ and $AR_{cbl20–30}/AR_{MCA20–30}$ on ^{99m}Tc-ECD SPECT for detecting abnormally elevated AR_{MCA} on OEF PET in patients. The area under the ROC curve is significantly greater for $AR_{cbl20–30}/AR_{MCA20–30}$ than for $AR_{MCA20–30}$ (difference between areas, 0.167; $P = 0.0001$).

ROC curve was significantly greater for $AR_{cbl20–30}/AR_{MCA20–30}$ (0.947 [95% CI, 0.882–0.982]) than for $AR_{MCA20–30}$ (0.780 [95% CI, 0.685–0.858]) (difference between areas, 0.167; $P = 0.0001$).

Figure 3 and Table 2 show the sensitivity, specificity, and positive and negative predictive values for $AR_{MCA20–30}$ and $AR_{cbl20–30}/AR_{MCA20–30}$ on ^{99m}Tc-ECD SPECT at the cutoff point (0.952 for $AR_{MCA20–30}$; 1.062 for $AR_{cbl20–30}/AR_{MCA20–30}$) that was closest to the left upper corner of the ROC curve for detecting abnormally elevated AR_{MCA} on OEF PET. The sensitivity and negative predictive value were 100% for both $AR_{MCA20–30}$ and $AR_{cbl20–30}/AR_{MCA20–30}$. Although the positive predictive value was not significantly different between $AR_{MCA20–30}$ and $AR_{cbl20–30}/AR_{MCA20–30}$, the specificity was significantly greater for the latter than for the former.

When the abnormally reduced $AR_{MCA20–30}$ on ^{99m}Tc-ECD SPECT was defined as a value lower than the cutoff point, 0.952, obtained in the ROC analysis, 47 of 97 patients studied were defined as having abnormally reduced $AR_{MCA20–30}$ on ^{99m}Tc-ECD SPECT. For these 47 patients, the sensitivity, specificity, and positive and negative predictive values for $AR_{cbl20–30}/AR_{MCA20–30}$ at the cutoff point that was closest to the left upper corner of the ROC curve for detecting abnormally elevated AR_{MCA} on OEF PET are shown in Table 2. The positive predictive value was significantly greater for $AR_{cbl20–30}/AR_{MCA20–30}$ for patients with abnormally reduced $AR_{MCA20–30}$ than for $AR_{MCA20–30}$ alone.

Representative ^{15}O gas PET and ^{99m}Tc-ECD SPECT images in a patient with unilateral ICA occlusion and abnormally elevated AR_{MCA} on OEF PET are shown in Figure 5.

DISCUSSION

The present study demonstrated that a combination of asymmetries in the cerebellar and cerebral hemispheres on ^{99m}Tc-ECD SPECT with a scan time of 20 to 30 minutes after tracer administration optimally detects misery perfusion in unilateral ICA or MCA occlusive disease.

To display CBF images using ^{99m}Tc-ECD SPECT in clinical settings, data acquisition is commonly started 5 to 60 minutes after tracer administration with a scanning duration of 10 to 20 minutes.[13,20–26] Our data showed that the optimal scan time to display affected-to-contralateral side asymmetry of CBF in the cerebral hemispheres on ^{99m}Tc-ECD SPECT was 20 to 30 minutes after tracer administration. However, the affected-to-contralateral side asymmetry even with this scan time was underestimated in comparison with that on CBF PET in most patients, corresponding to previous findings that ^{99m}Tc-ECD accumulation has a nonlinear relationship with the true CBF.[13,20–26] Limited extraction is likely important in this nonlinear relationship,[13] which is present because of the fairly small permeability–surface area product.[21,27] ^{99m}Tc-ECD demonstrates not only rapid blood clearance, but also fast conversion of the original lipophilic compound to hydrophilic breakdown products in the blood and brain.[28] For this reason, arterial input to the brain is small during the short amount of time after intravenous administration of the tracer. Limited extraction decreases radioactivity in regions with high blood flow.[13]

A previous study demonstrated that although contralateral-to-affected side asymmetry in the cerebellar hemispheres on CBF PET is correlated with affected-to-contralateral side asymmetry in the cerebral hemispheres on $CMRO_2$ PET, the correlation coefficient is considerably higher when reanalyzed only in patients undergoing a PET study within 3 months after the last ischemic episode.[11] Crossed cerebellar hypoperfusion is often not observed in patients with decreased $CMRO_2$ in the cerebral hemisphere on the same side as occlusion of a major cerebral artery.[29] Crossed

TABLE 2. Sensitivity, Specificity, and Positive and Negative Predictive Values for AR_{MCA} Versus $AR_{cbl20–30}/AR_{MCA20–30}$ or $AR_{cbl20–30}/AR_{MCA20–30}$ for Only Abnormally Reduced $AR_{MCA20–30}$ on ECD SPECT to Detect Misery Perfusion

	A	B	C	Significant Difference*	
	$AR_{MCA20–30}$ (n = 97)	$AR_{cbl20–30}/AR_{MCA20–30}$ (n = 97)	$AR_{cbl20–30}/AR_{MCA20–30}$ for Abnormally Reduced $AR_{MCA20–30}$ (n = 47)	A vs B	A vs C
Sensitivity	100.0% (17/17)	100.0% (17/17)	100.0% (17/17)	No	No
95% CI	100.0%–100.0%	100.0%–100.0%	100.0%–100.0%		
Specificity	62.5% (50/80)	86.3% (69/80)	73.3% (22/30)	Yes	No
95% CI	51.9%–73.1%	78.7%–93.8%	57.5%–89.2%		
Positive predictive value	36.2% (17/47)	60.7% (17/28)	68.0% (17/25)	No	Yes
95% CI	22.4%–49.7%	42.6%–78.8%	49.9%–86.3%		
Negative predictive value	100.0% (50/50)	100.0% (69/69)	100.0% (22/22)	No	No
95% CI	100.0%–100.0%	100.0%–100.0%	100.0%–100.0%		
Cutoff point	0.952	1.062	1.062		

*Differences are analyzed using the 95% CI.

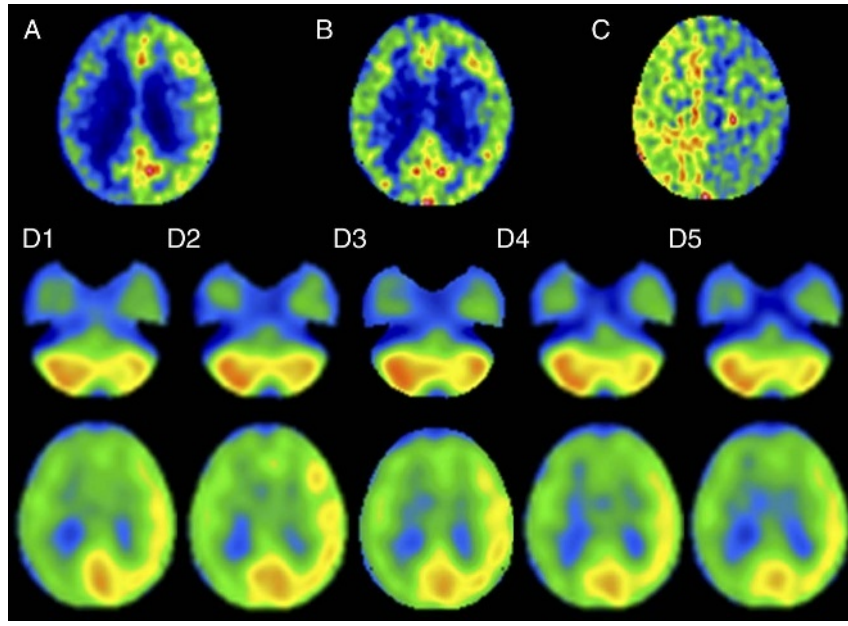

FIGURE 5. A 66-year-old man with symptomatic occlusion of the right ICA. Upper images, ^{15}O gas PET images including CBF (**A**), $CMRO_2$ (**B**), and OEF (**C**). Although CBF is lower in the right cerebral hemisphere than in the left cerebral hemisphere, the degree of asymmetry in $CMRO_2$ is less, resulting in considerably greater OEF in the right cerebral hemisphere than in the left cerebral hemisphere. **D1** to **D5**, ^{99m}Tc-ECD SPECT images at 0 to 10 minutes, 10 to 20 minutes, 20 to 30 minutes, 30 to 40 minutes, and 40 to 50 minutes (**D1**–**D5**) after tracer administration. Tracer uptake is lower in the right cerebral hemisphere than in the left cerebral hemisphere and in the left cerebellar hemisphere than in the right cerebellar hemisphere at all scan times after tracer administration. The degree of the asymmetry appears to be greater on images with a scan time of 10 to 20 minutes and 20 to 30 minutes after tracer administration than with other scan times.

cerebellar hypoperfusion often resolves 2 to 3 months after hypertensive putaminal hemorrhage.[30] Thus, although CCH basically shows $CMRO_2$ asymmetry in the cerebral hemisphere, this phenomenon may disappear over the course of several months after a supratentorial cerebrovascular event, even though $CMRO_2$ asymmetry persists.[11] Thus, our study included only patients undergoing PET and SPECT studies within 3 months after the last ischemic episode. As a result, contralateral-to-affected side asymmetry in the cerebellar hemispheres on ^{99m}Tc-ECD SPECT was correlated with affected-to-contralateral side asymmetry in the cerebral hemispheres on $CMRO_2$ PET. This relationship corresponded with results comparing CBF and $CMRO_2$ on PET.[10,11] Our data also showed that the optimal scan time to infer affected-to-contralateral side asymmetry of $CMRO_2$ in the cerebral hemispheres using ^{99m}Tc-ECD SPECT was 20 to 30 minutes after tracer administration. This scan time was conveniently identical to the optimal scan time required to display affected-to-contralateral side asymmetry of CBF in the cerebral hemispheres on ^{99m}Tc-ECD SPECT.

In the present study, abnormal elevation of OEF in the affected hemisphere relative to OEF in the contralateral hemisphere was defined as misery perfusion in the affected hemisphere, and abnormally elevated AR_{MCA} on OEF PET was defined as a value greater than the mean ± 2 SDs (1.089) of the normal values. Patients showing AR_{MCA} greater than 1.082 on OEF PET due to unilateral ICA steno-occlusive disease were considered to have misery perfusion and are at high risk of stroke.[31] In our study, the cutoff point for AR_{MCA} on OEF PET was similar to that of Grubb et al.[31] Our study demonstrated that affected-to-contralateral side asymmetry in the cerebral hemispheres on ^{99m}Tc-ECD SPECT was correlated with asymmetry on OEF PET and detected misery perfusion with sensitivity and a negative predictive value of 100% at the cutoff point of 0.952. These findings corresponded to the principle that a cerebral hemisphere with misery perfusion due to unilateral ICA or MCA occlusive disease has reduced CBF in the affected hemisphere.[5] Furthermore, the ratio of contralateral-to-affected side asymmetry in the cerebellar hemispheres to affected-to-contralateral side asymmetry in the cerebral hemispheres on ^{99m}Tc-ECD SPECT detected misery perfusion with high accuracy, with an area under the ROC curve of greater than 0.9. This accuracy was significantly higher for the ratio than for affected-to-contralateral side asymmetry in the cerebral hemispheres on ^{99m}Tc-ECD SPECT. These findings demonstrated that the combination of asymmetries in the cerebellar and cerebral hemispheres on ^{99m}Tc-ECD SPECT optimally detects misery perfusion.

Our study also showed that the additional calculation of cerebellar asymmetry for patients with strong cerebral asymmetry (AR_{MCA} <0.952) on ^{99m}Tc-ECD SPECT significantly increased the positive predictive value for the detection of misery perfusion. Based on our data, we suggest the following clinical algorithm for optimal detection of misery perfusion using ^{99m}Tc-ECD SPECT: A patient with unilateral ICA or MCA occlusive disease undergoes ^{99m}Tc-ECD SPECT with a scan time of 20 to 30 minutes after tracer administration. If strong cerebral asymmetry is observed, cerebellar asymmetry is calculated next. A patient with a high ratio of cerebellar asymmetry to cerebral asymmetry (AR_{cbl}/AR_{MCA} >1.062) is finally determined to probably have misery perfusion in the affected hemisphere.

Our study has several limitations. First, patients with subcortical infarctions have not only primary ischemic cortical damage but also cerebral cortical hypometabolism because of transneuronal mechanisms and cerebrocerebellar tract damage, which lead to CCH.[10] Deep infarcts injuring the internal capsule especially induce severe CCH.[9] In patients with unilateral ICA or MCA steno-occlusive disorder in whom the infarction is restricted to the

posterior limb of the internal capsule, CCH without hypometabolism in the ipsilateral cerebral cortex still occurs.[10,32] We excluded patients with subcortical infarctions that affect the posterior limb of the internal capsule, and our results are not applicable to such patients. Second, as mentioned previously, our study included only patients undergoing PET and SPECT studies within 3 months after the last ischemic episode. Whether a combination of asymmetries in the cerebellar and cerebral hemispheres on ^{99m}Tc-ECD SPECT detects misery perfusion in patients in whom more than 3 months has elapsed after the last ischemic episode remains unknown.

CONCLUSIONS

The present study demonstrated that the combination of asymmetries in the cerebellar and cerebral hemispheres on ^{99m}Tc-ECD SPECT with a scan time of 20 to 30 minutes after tracer administration optimally detects misery perfusion in unilateral major cerebral artery occlusive disease.

REFERENCES

1. Baron JC, Bousser MG, Rey A, et al. Reversal of focal "misery-perfusion syndrome" by extra-intracranial arterial bypass in hemodynamic cerebral ischemia. A case study with ^{15}O positron emission tomography. *Stroke*. 1981; 12:454–459.
2. Yamauchi H, Higashi T, Kagawa S, et al. Is misery perfusion still a predictor of stroke in symptomatic major cerebral artery disease? *Brain*. 2012;135: 2515–2526.
3. Sato Y, Ogasawara K, Kuroda H, et al. Preoperative central benzodiazepine receptor binding potential and cerebral blood flow images on SPECT predict development of new cerebral ischemic events and cerebral hyperperfusion after carotid endarterectomy. *J Nucl Med*. 2011;52:1400–1407.
4. Kawai N, Hatakeyama T, Okauchi M, et al. Cerebral blood flow and oxygen metabolism measurements using positron emission tomography on the first day after carotid artery stenting. *J Stroke Cerebrovasc Dis*. 2014;23: e55–e64.
5. Powers WJ. Cerebral hemodynamics in ischemic cerebrovascular disease. *Ann Neurol*. 1991;29:231–240.
6. Komaba Y, Mishina M, Utsumi K, et al. Crossed cerebellar diaschisis in patients with cortical infarction: logistic regression analysis to control for confounding effects. *Stroke*. 2004;35:472–476.
7. Takasawa M, Watanabe M, Yamamoto S, et al. Prognostic value of subacute crossed cerebellar diaschisis: single-photon emission CT study in patients with middle cerebral artery territory infarct. *AJNR Am J Neuroradiol*. 2002; 23:189–193.
8. Baron JC, Bousser MG, Comar D, et al. "Crossed cerebellar diaschisis": a remote functional suppression secondary to supratentorial infarction in man. *J Cereb Blood Flow Metab*. 1981;1:s500.
9. Pantano P, Baron JC, Samson Y, et al. Crossed cerebellar diaschisis. Further studies. *Brain*. 1986;109:677–694.
10. Yamauchi H, Fukuyama H, Yamaguchi S, et al. Crossed cerebellar hypoperfusion in unilateral major cerebral artery occlusive disorders. *J Nucl Med*. 1992;33:1637–1641.
11. Matsumoto Y, Ogasawara K, Saito H, et al. Detection of misery perfusion in the cerebral hemisphere with chronic unilateral major cerebral artery stenoocclusive disease using crossed cerebellar hypoperfusion: comparison of brain SPECT and PET imaging. *Eur J Nucl Med Mol Imaging*. 2013;40: 1573–1581.
12. Shimosegawa E, Hatazawa J, Aizawa Y, et al. Technetium-99m–ECD brain SPECT in misery perfusion. *J Nucl Med*. 1997;38:791–796.
13. Kado H, Iida H, Kimura H, et al. Brain perfusion SPECT study with ^{99m}Tc-bicisate: clinical pitfalls and improved diagnostic accuracy with a combination of linearization and scatter-attenuation correction. *Ann Nucl Med*. 2001;15:123–129.
14. Ibaraki M, Miura S, Shimosegawa E, et al. Quantification of cerebral blood flow and oxygen metabolism with 3-dimensional PET and ^{15}O: validation by comparison with 2-dimensional PET. *J Nucl Med*. 2008;49:50–59.
15. Frackowiak RS, Lenzi GL, Jones T, et al. Quantitative measurement of regional cerebral blood flow and oxygen metabolism in man using ^{15}O and positron emission tomography: theory, procedure, and normal values. *J Comput Assist Tomogr*. 1980;4:727–736.
16. Lammertsma AA, Jones T. Correction for the presence of intravascular oxygen-15 in the steady-state technique for measuring regional oxygen extraction ratio in the brain: 1. description of the method. *J Cereb Blood Flow Metab*. 1983;3:416–424.
17. Nishimiya M, Matsuda H, Imabayashi E, et al. Comparison of SPM and NEUROSTAT in voxelwise statistical analysis of brain SPECT and MRI at the early stage of Alzheimer's disease. *Ann Nucl Med*. 2008;22: 921–927.
18. Takeuchi R, Matsuda H, Yoshioka K, et al. Cerebral blood flow SPET in transient global amnesia with automated ROI analysis by 3DSRT. *Eur J Nucl Med Mol Imaging*. 2004;31:578–589.
19. Pepe MS, Longton G. Standardizing diagnostic markers to evaluate and compare their performance. *Epidemiology*. 2005;16:598–603.
20. Yonekura Y, Ishizu K, Okazawa H, et al. Simplified quantification of regional cerebral blood flow with ^{99m}Tc-ECD SPECT and continuous arterial blood sampling. *Ann Nucl Med*. 1996;10:177–183.
21. Yonekura Y, Tsuchida T, Sadato N, et al. Brain perfusion SPECT with ^{99m}Tc-bicisate: comparison with PET measurement and linearization based on permeability–surface area product model. *J Cereb Blood Flow Metab*. 1994;14:S58–S65.
22. Shishido F, Uemura K, Murakami M, et al. Cerebral uptake of ^{99m}Tc-bicisate in patients with cerebrovascular disease in comparison with CBF and $CMRO_2$ measured by positron emission tomography. *J Cereb Blood Flow Metab*. 1994;14:S66–S75.
23. Ito H, Inoue K, Goto R, et al. Database of normal human cerebral blood flow measured by SPECT: I. Comparison between I-123-IMP, Tc-99m-HMPAO, and Tc-99m-ECD as referred with O-15 labeled water PET and voxel-based morphometry. *Ann Nucl Med*. 2006;20:131–138.
24. Ishizu K, Yonekura Y, Magata Y, et al. Extraction and retention of technetium-99m-ECD in human brain: dynamic SPECT and oxygen-15-water PET studies. *J Nucl Med*. 1996;37:1600–1604.
25. Tsuchida T, Nishizawa S, Yonekura Y, et al. SPECT images of technetium-99m–ethyl cysteinate dimer in cerebrovascular diseases: comparison with other cerebral perfusion tracers and PET. *J Nucl Med*. 1994; 35:27–31.
26. Ma J, Mehrkens JH, Holtmannspoetter M, et al. Perfusion MRI before and after acetazolamide administration for assessment of cerebrovascular reserve capacity in patients with symptomatic internal carotid artery (ICA) occlusion: comparison with ^{99m}Tc-ECD SPECT. *Neuroradiology*. 2007; 49:317–326.
27. Tsuchida T, Yonekura Y, Nishizawa S, et al. Nonlinearity correction of brain perfusion SPECT based on permeability–surface area product model. *J Nucl Med*. 1996;37:1237–1241.
28. Walovitch RC, Hill TC, Garrity ST, et al. Characterization of technetium-99m-L,L-ECD for brain perfusion imaging, part 1: pharmacology of technetium-99m ECD in nonhuman primates. *J Nucl Med*. 1989;30: 1892–1901.
29. Martin WR, Raichle ME. Cerebellar blood flow and metabolism in cerebral hemisphere infarction. *Ann Neurol*. 1983;14:168–176.
30. Ishikawa Y, Mukawa J, Kinjo T, et al. Crossed cerebellar diaschisis in putaminal hemorrhage—evaluation by the Xe-133 clearance method. *No To Shinkei*. 1994;46:335–340.
31. Grubb RL Jr, Derdeyn CP, Fritsch SM, et al. Importance of hemodynamic factors in the prognosis of symptomatic carotid occlusion. *JAMA*. 1998; 280:1055–1060.
32. Pappata S, Mazoyer B, Tran Dinh S, et al. Effects of capsular or thalamic stroke on metabolism in the cortex and cerebellum: a positron tomography study. *Stroke*. 1990;21:519–524.